Theoretical and Numerical Analysis of Polarization for Time Dependent Radiative Transfer Equations

Guillaume Bal

Department of Mathematics, University of Chicago, Chicago, IL 60637, USA
gbal@math.uchicago.edu

Miguel Moscoso *

Department of Mathematics, Stanford University, Stanford, USA
mmoscoso@math.stanford.edu

Abstract

We consider the matrix-valued radiative transfer equations for the Stokes parameters for the propagation of light through turbulent atmospheres. A Monte Carlo method is introduced to solve the time dependent matrix-valued radiative transfer equations in 3D geometry. The Monte Carlo method is based on a probabilistic representation of the radiative transfer equations involving an augmented scalar transport equation where the polarization parameters are independent variables. The linear moments of the augmented transport equation with respect to the polarization parameters solve the matrix-valued radiative transfer equations. We show how polarization and depolarization effects develop in time for isotropic and unpolarized point sources, considered for concreteness in spherical and half space geometries. We analyze in detail the creation of polarization by single scattering and multiple scattering effects.

1 Introduction

Electromagnetic wave propagation in weakly fluctuating random media over distances long compared to the wavelength can be described by radiative transfer equations [1–3]. Although light has a vector nature, this is often neglected and the matrix-valued radiative transfer equation is replaced by a scalar radiative transfer equation. The simplification amounts to neglecting the polarized

* To whom all correspondence should be addressed.

nature of light and is usually used when the source of light is unpolarized and only the total intensity is of interest. However, several authors [4,5] have shown that in the steady state case the error for the intensity caused by neglecting the polarized nature of light can be very large. A more accurate description of light propagation is then necessary. Even though there exist more accurate scalar equations [6], we consider here the full matrix-valued equations for the Stokes parameters.

Another interesting application of the matrix-valued radiative transfer equations is to characterize and compute the degree of polarization. Even in the case where the error on the intensity in the scalar approximation is acceptable, we will show that the degree of polarized light can still be large. This additional information may be valuable in solving some inverse problems more accurately, for instance in remote sensing [7,8] or medical diagnostics [9,10].

We are aiming at presenting a general and relatively easy to implement method for solving time dependent matrix-valued radiative transfer equations in 3D geometries based on a Monte Carlo method. It is well known that scalar equation have a straightforward probabilistic representation suitable for Monte Carlo simulations [11–13]. Unlike scalar equations however, matrix-valued equations do not have the same direct probabilistic representation. We follow the probabilistic representation of polarized radiative transfer equations given in [14], which involves an augmented scalar transport equation where the polarization parameters become independent variables. The main interest of the augmented transport is that its linear moments with respect to the polarization parameters solve the matrix-valued radiative transfer equations.

We are interested here in transient phenomena generated by pulsed sources. Characteristic times range in practice from hundreds of picoseconds in time-resolved ultrafast laser technology [15] to hundreds of seconds in seismology [16]. There is in general no analytical solution to the full radiative transfer equation. However, the single scattering approximation can be computed analytically. This provides us with a good understanding of how polarization is generated by scattering. It is also known that for large times, where multiple scattering is dominant, a decay in the rate of polarization takes place [17]. We show here the exact decay of polarization in the simplified case of a homogeneous medium. For more complicated geometries, we present Monte Carlo simulations of the matrix-valued radiative transfer equation and analyze the behavior in time of polarization and depolarization effects. Our source term is assumed to be a delta function in time and space and to be isotropic, i.e. spherically symmetric. We consider here two geometries. The first one is spherical and a partial theoretical analysis in presented. The second geometry is a half space. We consider it in order to understand the effect of boundaries or interfaces on the degree of polarization.

Our paper is organized as follows. In section 2 we recall the system of radiative transfer equation for electromagnetic waves. Next we show how to solve this system by a Monte Carlo method. This requires the construction of an augmented radiative transfer process. In section 3 we first address the creation of polarization by single scattering of a isotropic delta source term in spherical geometry, and second the cancellation of polarization by multiple scattering in homogeneous domains, i.e. domains without spatial dependence. We give in section 4 the main steps of the implementation of the Monte Carlo method. We present our numerical results in section 5. First we show the evolution of the electromagnetic wave energy in the full space. Then, we consider the half space problem and show how the polarization parameters are affected by the presence of an interface. We summarize our results in the concluding section 6.

2 Radiative Transfer Equations for Electromagnetic Waves

2.1 Radiative Transfer Equation

We consider the propagation of electromagnetic waves in random media with weak fluctuations of the dielectric permitivity and correlation length comparable to the wavelength. The electromagnetic wave energy density solves then a matrix-valued radiative transfer equation [17]. More general radiative transfer equations can be dealt with [18–21]. The evolution of energy density in phase space is described by a 2×2 coherence matrix $W(t,x,k)$, which is related to the Stokes parameters I, Q, U, V, see [1,17], by

$$W(t,x,k) = \frac{1}{2}\begin{pmatrix} I+Q & U+iV \\ U-iV & I-Q \end{pmatrix}. \tag{1}$$

The parameter I describes the total intensity of the electromagnetic wave energy, whereas Q, U, and V describe its polarization. A scalar measure to quantify the amount of polarized energy density to the total amount of energy density is given by the *degree of polarization*

$$\alpha(t,x,k) = \sqrt{\frac{Q^2(t,x,k)+U^2(t,x,k)+V^2(t,x,k)}{I^2(t,x,k)}}\,, \tag{2}$$

which takes values between 0 (for unpolarized waves) and 1 (for fully polarized waves).

The radiative transfer equation for W takes the form

$$\frac{1}{v}\frac{\partial W(t,x,k)}{\partial t} + \hat{k}\cdot\nabla_x W(t,x,k) = \tag{3}$$
$$\int \sigma(k,k')T(k,k')W(t,x,k')T^*(k,k')\delta(v|k|-v|k'|)\,dk' - \Sigma(k)W(t,x,k).$$

Here v denotes the velocity of propagation of light inside the medium. The scattering is elastic. Therefore, in a lossless medium, we have that the total cross section Σ satisfies

$$\Sigma(k)\mathbb{I}_2 = \int \sigma(k',k)T(k',k)\mathbb{I}_2 T^*(k',k)\delta(v|k|-v|k'|)dk', \tag{4}$$

where $\mathbb{I}_2$ is the 2×2 identity matrix, and

$$\sigma(k,k') = \frac{\pi}{2}v^2|k|^2\hat{R}_\varepsilon(k-k'), \tag{5}$$

is a scalar function given in terms of the power spectral density function $\hat{R}_\varepsilon$. The power spectral density function is defined as the Fourier transform of the two point correlation function of the fractional permittivity fluctuations [17]. For simplicity we assume that $\hat{R}_\varepsilon$ is identically equal to a constant. This correspond to the so called Rayleigh scattering, which is used to model the scattering of light in a turbulent atmosphere [1]. We then obtain that the total cross section Σ in (4) is constant. The 2×2 matrix $T(k,k')$ is defined by

$$T_{ij}(k,k') = (z^{(i)}(k)\cdot z^{(j)}(k')), \tag{6}$$

with the vectors $(\hat{k}, z^{(1)}(k), z^{(2)}(k))$,

$$\hat{k} = \begin{pmatrix}\sin\theta\cos\phi\\ \sin\theta\sin\phi\\ \cos\theta\end{pmatrix},\ z^{(1)}(k) = \begin{pmatrix}\cos\theta\cos\phi\\ \cos\theta\sin\phi\\ -\sin\theta\end{pmatrix},\ z^{(2)}(k) = \begin{pmatrix}-\sin\phi\\ \cos\phi\\ 0\end{pmatrix}, \tag{7}$$

forming an orthonormal basis in $\mathbb{R}^3$. We have denoted by T^* the transpose matrix of T. Note that $T^*(k,k') = T(k',k)$. Moreover the vector $z^{(2)}(k)$ is uniquely defined for all vectors k such that $|k\cdot e_z| < 1$, where e_z is the third vector in the basis where the vectors (7) are represented. It is important to observe that the coherence matrix W as well as the radiative transfer equation (3) are represented in a given orthonormal basis (e_x, e_y, e_z). The change of representation by rotation of the basis is not straightforward; we refer to [1] and section 5.1.1 to see how the polarization parameters are changed by rotation.

We note that the frequency $\omega = v|k|$ of the energy density is conserved by the free transport operator on the left-hand side of (3) and by the elastic scattering operator on the right-hand side of (3). Therefore, the equations for different frequencies are uncoupled. We consequently assume that the modulus $|k|$ is fixed.

The initial condition we consider in this paper is an unpolarized isotropic source term of the form $W_0(x,k) = w_0 \mathrm{I\!I}_2 \delta(x)$. Let us define the following adimensionalized quantity

$$\tilde{W}(t,x,k) = \frac{1}{w_0} W(\frac{t}{v\Sigma}, \frac{x}{\Sigma}, \frac{\omega k}{v}). \tag{8}$$

We then recast (3) as

$$\frac{\partial \tilde{W}}{\partial t} + \hat{k} \cdot \nabla_x \tilde{W}(t,x,k) = \frac{3}{8\pi} \int_{|k'|=1} T(k,k')\tilde{W}(t,x,k')T^*(k,k')\, dk' - \tilde{W}(t,x,k), \tag{9}$$

with initial condition $\tilde{W}(0,x,k) = \mathrm{I\!I}_2 \delta(x)$. In the sequel, we drop the symbol $\tilde{}$ for simplicity. Let us point out that the real and imaginary parts of W are uncoupled since the matrix T is real. Therefore, V satisfies an independent equation and we assume without loss of generality that $V = 0$, which corresponds to linearly polarized waves.

2.2 Probabilistic Representation and Augmented Transport

We want to solve (9) by a Monte Carlo method. This method, although slowly convergent, enables us to deal with complicated 3D geometries with reasonable storage requirements and is in addition relatively easy to implement. For this reason, it is very popular in radiation transport, heat transfer, and nuclear reactor theory [12,13]. The radiative transfer equations for scalar waves have the same structure as transport equations for particles. The central characteristic of Monte Carlo methods is to simulate the behavior of one particle at a time. The average over a large number of realizations of particle paths yields an estimate of the particle probability density.

The simulation of the particle trajectories is threefold. First, we describe the particle trajectories between successive scattering events. Then, we calculate the time of the next scattering with the underlying medium. Finally, at the time when the particle undergoes scattering, we compute its outgoing velocity. The last two steps, time of scattering and outgoing velocity after scattering, are random processes.

As it stands, this method is not valid for coherence matrices, whose entries do not necessarily correspond to energies but include polarization parameters.

Moreover, the probability distribution of the outgoing velocity after scattering does not depend only on the incident direction, as for scalar particle transport, but also on its polarization state.

Nonetheless, it is possible to devise a probabilistic representation for polarized wave transport by considering the polarization parameters as independent variables. We follow here a recent derivation given in [14] which we also applied to the propagation of seismic waves in the Earth crust [22]. We first have to introduce a transport process for the energy density resolved not only over directions but also over the polarization states. For its derivation it is convenient to rewrite the matrix W as

$$W(t,x,k) = \frac{I}{2}\begin{pmatrix} 1+Q/I & U/I \\ U/I & 1-Q/I \end{pmatrix} = \frac{I}{2}\left[\mathbb{I}_2 + \mathcal{P}\right] \, , \tag{10}$$

where

$$\mathcal{P} = \begin{pmatrix} p_1 & p_2 \\ p_2 & -p_1 \end{pmatrix} = \begin{pmatrix} Q/I & U/I \\ U/I & -Q/I \end{pmatrix} \, , \tag{11}$$

and $\mathbb{I}_2$ is the 2×2 identity matrix. Note that the intensity I is the trace of $W(t,x,k)$. In addition to the position $X(t)$ and wave vector (velocity) $K(t)$ we now have a pair of polarization processes $p_1(t)$ and $p_2(t)$ which describe the polarization parameters Q and U, see (11). The position $X(t)$ is continuous in space, while the velocity and polarization parameters $Y(t) = (K(t), \mathcal{P}(t))$ jump at the scattering times.

The evolution of the jump process $(X(t), K(t), \mathcal{P}(t))$ follows the following rules. The process evolves along straight characteristics between successive scattering:

$$\frac{dX}{dt} = K(t), \qquad \frac{dK}{dt} = 0, \qquad \frac{dp_i}{dt} = 0, \quad i = 1, 2. \tag{12}$$

At time s, the probability that the next scattering takes place after time t follows the Poisson distribution

$$P(\text{Time of Next Scattering} > t) = e^{-(t-s)}. \tag{13}$$

When a scattering event takes place, we have to define the probability of the outgoing velocity and polarization parameters. The probability density for a jump from wave vector k and polarization matrix $\mathcal{P}$ into wave vector k' and polarization matrix $\mathcal{P}'$ is

$$\Pi(k, \mathcal{P}, k', \mathcal{P}') = \frac{3}{8\pi} \mathrm{Tr}\left\{T(k',k)[\mathbb{I}_2 + \mathcal{P}]T^*(k',k)\right\}. \tag{14}$$

The matrix of the scattered polarization parameters $\mathcal{P}_s(k, \mathcal{P}, k')$, which is symmetric and has null trace, is determined by [14]

$$\frac{1}{2}(\mathbb{I}_2 + \mathcal{P}_s) = \frac{T(k', k)[\mathbb{I}_2 + \mathcal{P}]T^*(k', k)}{\mathrm{Tr}\{T(k', k)[\mathbb{I}_2 + \mathcal{P}]T^*(k', k)\}}. \tag{15}$$

For the reader's convenience, we have postponed to Appendix A the computation of the probability measure Π and the scattered polarization parameters in the case of Rayleigh scattering. We see in these expressions that the jump probability does not depend upon the outgoing polarization parameters $\mathcal{P}'$ and that the outgoing polarization parameters are functions of the incoming and outgoing velocities k and k', and of the incoming polarization parameters $\mathcal{P}$.

The jump process is constructed as follows. The jump process $(X(t), K(t), \mathcal{P}(t))$ starts at $(x_0, k_0, \mathcal{P}^0)$. The time of first scattering τ_1 is given by the probability density (13). The process follows (12) between $0 \le t < \tau_1$. At τ_1 the process jumps to a new velocity and new polarization parameters $Y(\tau_1)$ according to (14) and (15). Notice that the position $X(t)$ is continuous, i.e. $X(\tau_1^+) = X(\tau_1^-)$. Then a new scattering time τ_2 is obtained according to (13). The process is continued in an obvious manner until a final time t_f.

To solve Eq.(9) by Monte Carlo, we first consider the augmented transport equation for the probability density function $\rho(t, x, k, p_1, p_2)$ of the jump process $(X(t), K(t), \mathcal{P}(t))$ starting at point $(x_0, k_0, \mathcal{P}^0)$, which is given by

$$\begin{aligned} \frac{\partial \rho}{\partial t} + \hat{k} \cdot \nabla_x \rho = & \frac{3}{8\pi} \int\limits_{|k'|=1} dk' \int dp_1' dp_2' \mathrm{Tr}\left\{T(k, k')[\mathbb{I}_2 + \mathcal{P}']T^*(k, k')\right\} \\ & \times \delta(\mathcal{P}' - \mathcal{P}_s(k, \mathcal{P}, k'))\rho(t, x, k', p_1', p_2') - \rho(t, x, k, p_1, p_2), \end{aligned} \tag{16}$$

with suitable initial data. This is the forward Kolmogorov equation associated with the random process $(X(t), K(t), \mathcal{P}(t))$. The usual theory of probabilistic representations of transport equations [11–13] applies to (16). We solve it by estimating the probability density the jump process $(X(t), K(t), \mathcal{P}(t))$ using a Monte Carlo method. The Monte Carlo method consists of generating independent realizations of the augmented process and in calculating the resulting discretized probability density.

The main property of the augmented equation, which justifies the construction of the complicated augmented process, is that its linear moments with respect to the polarization parameters,

$$W(t, x, k) = \int dp_1 dp_2\, \rho(t, x, k, p_1, p_2) \frac{\mathbb{I}_2 + \mathcal{P}}{2}, \tag{17}$$

give a solution of the coherent matrix transport equation (9). Namely, let $W(t,x,k)$ be the solution of (9) with the initial data $W(0,x,k) = W_0(x,k)$. We decompose the initial data as

$$W_0(x,k) = \frac{w_0(x,k)}{2}\begin{pmatrix} 1+p_1^0 & p_2^0 \\ p_2^0 & 1-p_1^0 \end{pmatrix} = \frac{w_0(x,k)}{2}\left[\mathbb{I}_2 + \mathcal{P}^0(x,k)\right],$$

with $w_0(x,k) = \mathrm{Tr} W_0(x,k)$. Then, $W(t,x,k)$ is given by (17) where ρ solves (16) with the initial condition

$$\rho(0,x,k,\mathcal{P}) = w_0(x,k)\delta(\mathcal{P} - \mathcal{P}^0(x,k)). \tag{18}$$

For instance, an isotropic unpolarized local pulse is generated by

$$\rho(0,x,k,\mathcal{P}) = w_0(x,k)\delta(\mathcal{P} - 0\times\mathbb{I}_2), \qquad \text{where} \qquad w_0(x,k) = \delta(x).$$

Let us summarize the main steps in solving (9) numerically. We first write an augmented scalar transport equation (16). Next, this equation is solved by Monte Carlo simulation. The probability density $\rho(t,x,k,p_1,p_2)$ is calculated by averaging over a large number of realizations that simulate the trajectories of elementary polarized electromagnetic waves propagating inside the medium. The solution W of the radiative transfer equation (9) is then obtained by averaging over the first order moments of ρ with respect to the polarization parameters (17).

3 Polarization and Depolarization

For long times, scalar transport equations have asymptotically a simpler form in which the directional behavior is known, in most cases even constant, and the spatial behavior solves a diffusion equation. We refer to [11,23] for more details. The solutions of transport equations with polarization effects also converge to that of diffusion equations, as was shown in [14,17] for instance. So we expect that polarization effects disappear in time. We can also check easily that matrices proportional to the identity do not solve (9), even for non-polarized initial conditions, i.e., for initial conditions proportional to the identity. This means that polarization is created in time by the interaction of the wave energy with the underlying medium. We give in this section two simple mechanisms that account for the creation and annihilation of polarization, respectively.

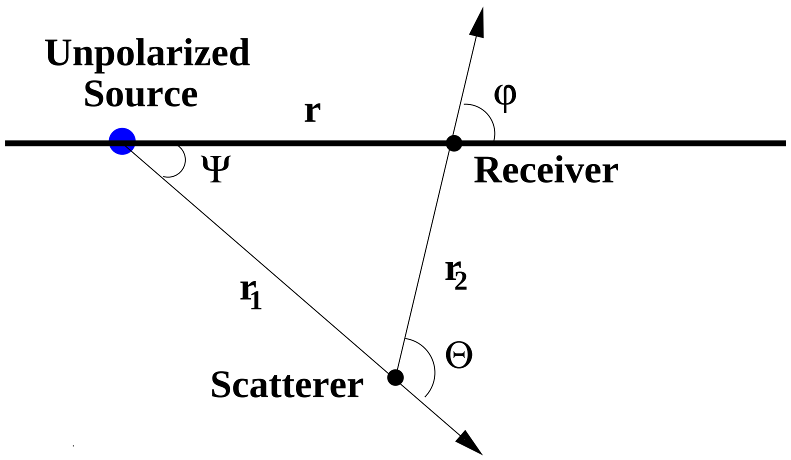

Fig. 1. Single scattering geometry.

3.1 Polarization and Single Scattering

The mechanism of creation of polarization is best understood by looking at the single scattering generated by a non polarized energy beam. For short times compared to the mean free time (the mean time between successive interactions with the medium, given by $(v\Sigma)^{-1} \equiv 1$ here), single scattering will dominate multiple scattering. Single scattering in spherical geometries has the main advantage that analytical expressions for the intensity and the degree of polarization can be worked out. In addition to being a fairly good approximation for short times, single scattering also provides a good understanding of how polarization is created when a source initially composed of natural light interacts with the underlying medium. We consider the case of spherically radiated natural light emitted by a delta source term in space and received at time t, after single scattering, at a point located at a distance r from the source. We calculate the spatio-temporal distribution of the intensity and the degree of polarization analytically. We use the relative simplicity of the spherical geometry in the analysis of the single scattering approximation; see Figure 1.

In this section we describe the scattering of light with the set of parameters [1]

$$J = (I_{||}, I_{\perp}, U),$$

instead of the Stokes parameters (I, Q, U). We have assumed here that $V = 0$. J is defined with respect to the scattering plane which contain the incident and scattered directions. $I_{||} = (I+Q)/2$ and $I_{\perp} = (I-Q)/2$ are the intensities parallel and perpendicular to the scattering plane, respectively.

Let Θ be the angle between the incident and scattered directions. Then, the scattered intensity in the direction Θ is proportional to RJ, where

$$R = \begin{pmatrix} \cos^2\Theta & 0 & 0 \\ 0 & 1 & 0 \\ 0 & 0 & \cos\Theta \end{pmatrix} . \tag{19}$$

For natural light, $I_{\|} = I_{\perp} = \frac{1}{2}I$ and $U = 0$. Therefore, the intensities of the scattered light in directions parallel and perpendicular respectively to the scattering plane are in the ratio $\cos^2\Theta$ to 1. Notice that the probability of being scattered in a direction making an angle Θ with the direction of incidence is the same for the coherence matrix radiative transfer equation and for the scalar approximation. Therefore, the intensities of the single scattering of natural light are identical in both equations. However, since polarization is obtained in the matrix-valued case, the intensity corresponding to second scattering will be different for the coherence matrix and the scalar approximation.

We see in Figure 1 that the intensity received at a time t in the direction φ, in a suitable system of coordinates, has been scattered at a point $\mathbf{r}_1$ making an angle Θ with the direction of the incident natural light. The relation between the scattering angle and $r_1 \equiv |\mathbf{r}_1|$ with φ is given by

$$\cos[\Theta(r,\varphi,t)] = \frac{2r^2 sin^2\varphi}{r^2 - 2rt\cos\varphi + t^2} - 1, \quad r_1 = \frac{r^2 - 2rt\cos\varphi + t^2}{2(t - r\cos\varphi)} . \tag{20}$$

For Rayleigh scattering, the intensity of the scattered light in right directions are in the ratio $\cos^2\Theta$ to 1 [1]. Then, the polarization of the intensity arriving with angle φ is given by

$$\alpha(r,\varphi,t) = \frac{1-\cos^2[\Theta]}{1+\cos^2[\Theta]} = \frac{1-(\frac{2r^2 sin^2\varphi}{r^2-2rt\cos\varphi+t^2} - 1)^2}{1+(\frac{2r^2 sin^2\varphi}{r^2-2rt\cos\varphi+t^2} - 1)^2} . \tag{21}$$

In Figure 2, we show the spatial distribution of the polarization after one scattering for different angles φ.

An averaged description of the polarization is obtained by defining the following degree of polarization:

$$\alpha_2(r,t) = \frac{1}{2}\int_0^\pi \alpha(r,\varphi,t) sin(\varphi) d\varphi . \tag{22}$$

A numerical computation of (22) is given in Figure 3. Observe that α_2 exactly vanishes at the source location. This is because the scattering angle is π for

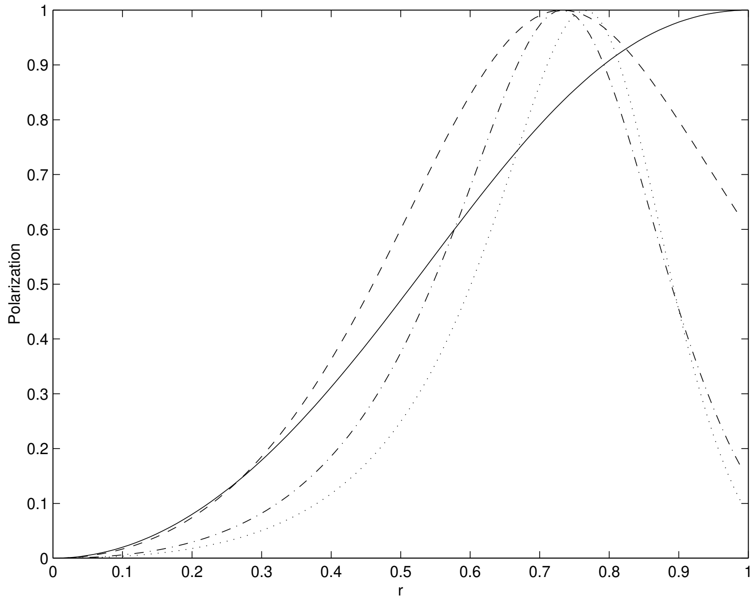

Fig. 2. Spatial distribution of the rate of polarization $\alpha_1(r, \varphi, 1)$ for $\varphi = \pi/2$ (solid line), $\varphi = \pi/3$ (dashed line), $\varphi = \pi/6$ (dash-dotted line) and $\varphi = \pi/8$ (dotted line).

all directions φ and because unpolarized beams scattered in the back direction remains unpolarized. We also see that the degree of polarization strongly depends on the distance to the source, and reaches its maximum value at $r/t \approx 3/4$. Although (22) is a natural averaged quantity over directions, we prefer to use

$$\alpha_1(r,t) = \frac{\int_0^\pi \alpha(r,\varphi,t) I(r,\varphi,t) sin(\varphi) d\varphi}{\int_0^\pi I(r,\varphi,t) sin(\varphi) d\varphi} \ , \tag{23}$$

where

$$I(r,\varphi,t) = \frac{1}{8\pi r_1 (t - r\cos\varphi)} \frac{3}{4} (1 + \cos^2\Theta), \tag{24}$$

is the intensity received in the direction φ. In (24) r_1 and Θ are given by (20). Equation (23) represents the percentage of diffuse energy which is fully polarized. The degree of polarization α_1 behaves better numerically than α_2 given in (22) because the directions with more particles, for which the resolution is better, are more represented. This will be particularly important for the long time computations presented in subsequent sections, where most of the particles remain close to the location of the source.

We show in Appendix B the derivation of (24) and the analytical integration

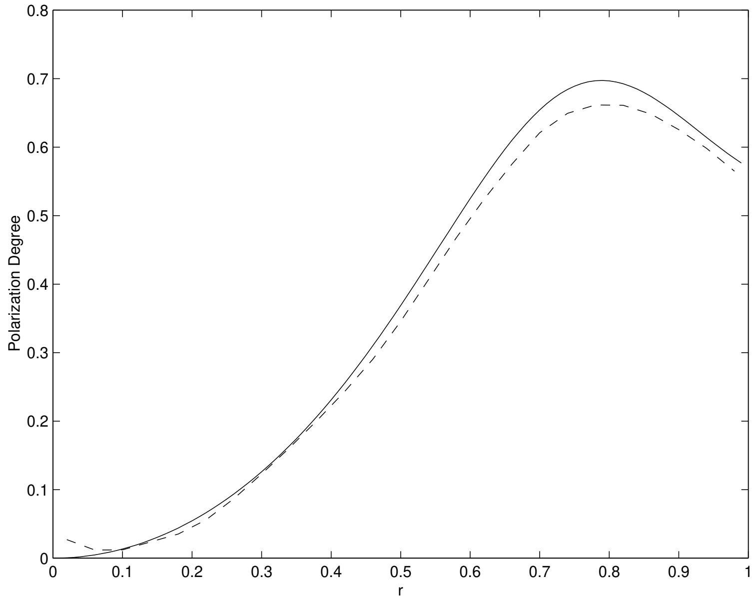

Fig. 3. Spatial distribution of $\alpha_2(r,1)$. The dashed curve is the numerical computation for a discrete number of directions $n_k = 12$; see section 5.1.

of $\alpha_1(r,t)$. Denoting by $\nu = t/r$, the result after computations is

$$\alpha_1(r,t) = \frac{3}{16\pi r^2}\frac{1}{I(r,t)}\{\frac{\nu^4+2\nu^2-3}{2\nu^5}\ln\frac{\nu+1}{\nu-1} - \frac{\nu^2-3}{\nu^4}\}, \tag{25}$$

where

$$I(r,t) = \frac{3}{16\pi r^2}\{\frac{3\nu^4-2\nu^2+3}{2\nu^5}\ln\frac{\nu+1}{\nu-1} + \frac{\nu^2-3}{\nu^4}\}\ , \tag{26}$$

is the total intensity for Rayleigh scattering. In equation (25), the rate $\alpha_1(r,t)$ is only a function of the ratio $\nu = t/r$ and reaches a maximum at $\nu_{max} = 1.27$ approximately; see Figure 4. Measurement of this maximal value could be used to determine the location of the source to a fixed receiver. Also, notice in Figure 4, where is represented the spatio-temporal distribution of α_1, that the maximal value of the degree of polarization is close to 0.8. This means that up to 80% of the light is polarized after the first scattering. Let us emphasize that the polarization of light takes place very quickly in terms of mean free times. Notice also that in equation (25), $\alpha_1(r,t)$ goes to 0 when $r \to t$.

For the sake of comparison, we have represented in Figure 5 the spatio-temporal distribution of the intensity for Rayleigh scattering given by (26) in solid line, and the intensity for isotropic scattering in dashed line. We see that in both cases, there is a logarithmic blow up of the intensity near $r = t$, as is typical for single scattering [16]. However, more intensity is concentrated for Rayleigh scattering in the vicinity of the source than for isotropic scatter-

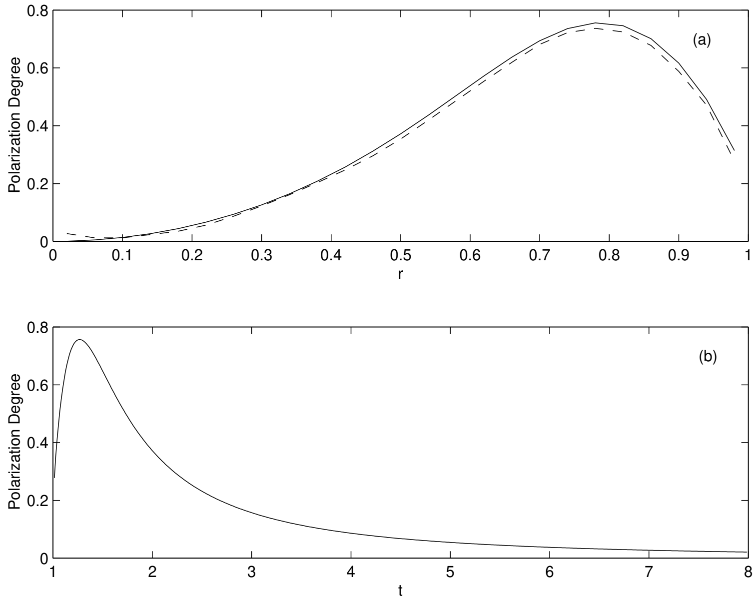

Fig. 4. (a) Spatial distribution $t = 1$ and (b) time evolution at $r = 1$ of the degree of polarization $\alpha_1(r, t)$ for the single scattering approximation. The dashed curve in (a) is the numerical computation for $n_k = 12$; see section 5.1.

ing. The difference between those two cases reaches up to 50% at the source location. We check that the asymptotic behavior of the total intensity in (26) is given for $r \ll t$ by $I(r, t) \approx 3/(4\pi t^2)$.

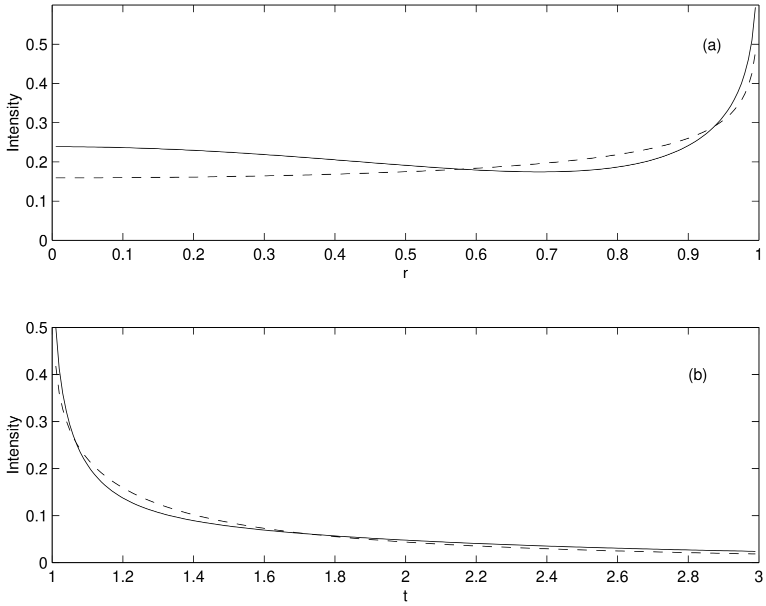

Fig. 5. (a) Spatial distribution at $t = 1$ and (b) time evolution of the intensity at $r = 1$ for the single scattering intensity $I(r, t)$ for Rayleigh (solid line) and isotropic (dashed line) scattering.

The mechanism responsible for the loss of polarization is multiple scattering. The same mechanism explains the regime of diffusion, where the energy density has the same value asymptotically in all directions of propagation. Diffusion theory implies that polarization effects and directional information disappear for long times and large distances of propagation; see [17] for instance. However, it remains difficult to quantify in practice how fast the decay really is and where the diffusive regime is valid. Before showing some numerical results, we present the simplest example of decay of polarization and directional information. We consider the propagation of light in a homogeneous medium with a homogeneous initial distribution of natural light. By homogeneous we mean space-independent. Moreover we assume that the initial distribution depends only on the polar angle θ and not the azimuthal angle ϕ, with respect to a given frame. Let $\mu = \cos\theta$. In this context, the radiative transfer equations (9) take the simpler form [1]

$$-\frac{\partial}{\partial t}\begin{pmatrix} I_l(t,\mu) \\ I_r(t,\mu) \end{pmatrix} = \begin{pmatrix} I_l(t,\mu) \\ I_r(t,\mu) \end{pmatrix} - \frac{3}{8}\int_{-1}^{1}\begin{pmatrix} 2(1-\mu^2)(1-\mu'^2)+\mu^2\mu'^2 & \mu^2 \\ \mu'^2 & 1 \end{pmatrix}\begin{pmatrix} I_l(t,\mu') \\ I_r(t,\mu') \end{pmatrix} d\mu', \quad (27)$$

where I_l and I_r are the apparent intensities in the two orthogonal directions l and r. They are related to I and Q by $I = I_l + I_r$ and $Q = I_l - I_r$. The asymptotic behavior of the solution for long times is obtained by solving the following spectral equation

$$\lambda\begin{pmatrix} I_l(t,\mu) \\ I_r(t,\mu) \end{pmatrix} = \begin{pmatrix} I_l(t,\mu) \\ I_r(t,\mu) \end{pmatrix} - \frac{3}{8}\int_{-1}^{1}\begin{pmatrix} 2(1-\mu^2)(1-\mu'^2)+\mu^2\mu'^2 & \mu^2 \\ \mu'^2 & 1 \end{pmatrix}\begin{pmatrix} I_l(t,\mu') \\ I_r(t,\mu') \end{pmatrix} d\mu'. \quad (28)$$

The scattering kernel in (27) is degenerate so there is a closed equation for a finite number of moments of I_l and I_r. Let us introduce

$$\phi_l^k(t) = \int_{-1}^{1} I_l(t,\mu)\mu^k d\mu \quad \text{and} \quad \phi_r^k(t) = \int_{-1}^{1} I_r(t,\mu)\mu^k d\mu.$$

We check that

$$(1-\lambda)\begin{pmatrix} I_l(t,\mu) \\ I_r(t,\mu) \end{pmatrix} = \frac{3}{8}\begin{pmatrix} 2(1-\mu^2)(\phi_l^0-\phi_l^2)+\mu^2(\phi_l^2+\phi_r^0) \\ \phi_l^2+\phi_r^0 \end{pmatrix}. \quad (29)$$

Upon taking three moments of this relation, we obtain

$$-\lambda \begin{pmatrix} \phi_l^0(t,\mu) \\ \phi_r^0(t,\mu) \\ \phi_l^2(t,\mu) \end{pmatrix} = \begin{pmatrix} 0 & 1/4 & -3/4 \\ 0 & -1/4 & 3/4 \\ 1/5 & 3/20 & -21/20 \end{pmatrix} \begin{pmatrix} \phi_l^0(t,\mu) \\ \phi_r^0(t,\mu) \\ \phi_l^2(t,\mu) \end{pmatrix}. \tag{30}$$

The possible values of λ are $0, 3/10$ and 1, which correspond to the eigenvectors $(3,3,1)$, $(15,-15,1)$ and $(1,-1,1)$ respectively. According to (29), the eigenvectors of (28) corresponding to 0 and $3/10$ are given, up to normalization, by

$$\begin{pmatrix} I_l^0(\mu) \\ I_r^0(\mu) \end{pmatrix} = \begin{pmatrix} 1 \\ 1 \end{pmatrix}, \qquad \begin{pmatrix} I_l^{-3/10}(\mu) \\ I_r^{-3/10}(\mu) \end{pmatrix} = \begin{pmatrix} 2-3\mu^2 \\ -1 \end{pmatrix}. \tag{31}$$

According to (29), we see that the eigenvalues of (28) different from -1 are 0 and $-3/10$. Therefore, defining $I = I_l + I_r$ and $Q = I_l - I_r$ where I_l and I_r solve (27), we have

$$\begin{aligned} I(t,\mu) &= \gamma + \beta(1-3\mu^2)\exp(-\frac{3t}{10}) + O(1)\exp(-t) \\ Q(t,\mu) &= 3\beta(1-\mu^2)\exp(-\frac{3t}{10}) + O(1)\exp(-t), \end{aligned} \tag{32}$$

where γ, and β are constants depending only on the initial conditions.

Let us make two remarks about polarization and depolarization effects. First, we can check that $Q(t,\mu) \equiv 0$ if $Q(0,\mu) = 0$. Therefore, no polarization is created in homogeneous media when the initial source is homogeneous. This is not true anymore for inhomogeneous initial source terms as we have see in section 3.1. Second, we can infer from the above analysis the rate of decay of the degree of polarization in regions where the intensity varies slowly. For Rayleigh scattering, the decay to diffusion behaves like $\exp -(3/10)t$. Moreover, we see from (32) that the loss of polarization and of directional information decay at the same rate. In other words, the second eigenvector $(I_l^{-3/10}, I_r^{-3/10})$ depends on μ and is partially polarized. We see that even in the case where the averaging is the fastest, the loss of polarization and of directional information is not very fast. It takes about 8 mean free times for a decay of the polarization by a factor 10.

4 Implementation of the Monte Carlo Method

In this section, we describe the implementation of the Monte Carlo method for solving the radiative transfer equation (9) using (16) and (17).

4.1 Decomposition in the number of scattering

Let us denote by

$$P(T, z, dz; z_0), \tag{33}$$

the probability that a particle starting at time 0 from $z_0 = (x_0, k_0, p_1^0, p_2^0)$ be at time T at $z = (x, k, p_1, p_2)$ about $dz = dx\, dk\, dp_1\, dp_2$. By definition of the probability density ρ solving (16) we have

$$P(T, z, dz; z_0) = \rho(T, z) dx\, dk\, dp_1\, dp_2.$$

The number of scattering events between 0 and T is finite (with probability one). Therefore, we can decompose $P(T, z, dz; z_0)$ over the number of scattering events as

$$P(T, z, dz; z_0) = \sum_{n=0}^{\infty} Pr(T, N_s = n) \times P(T, z, dz; z_0 | N_s = n), \tag{34}$$

where N_s is the number of scattering events, or jumps, of the process $(X(t), Y(t))$ between 0 and T. Here $|$ means conditional expectation and $Pr(T, N_s = n)$ is the probability of having exactly n scattering events between 0 and T. In other words, the total probability density is decomposed over the number of scattering events that the process suffers between 0 and T. The Poisson distribution of the law of scattering times (13) allows one to compute each term in the sum (34) separately by Monte Carlo method. We can check [24] that

$$Pr(T, N_s = n) = e^{-T} \frac{T^n}{n!}. \tag{35}$$

Moreover, for each number of scattering n, the times of scattering are obtained by increasing ordering of n values sampled between 0 and T with uniform distribution.

The first advantage in computing each term of the sum successively is the reduction of the statistical fluctuations. Indeed we include some information on the exact proportion of single scattering, double scattering, etc... in the total intensity. Moreover, we have access to those quantities and can easily obtain in which areas single scattering or multiple scattering is dominant. The second advantage is architectural. Our code is written in Matlab, which is much faster when properly vectorized. We calculate in turn the contributions of particles having exactly n scattering events during a fixed time T. Here, we have $1 \leq n \leq K$, where K is chosen so that the particles having more than K interactions during an interval of time of size T are negligible, i.e.

$$\sum_{n=K+1}^{\infty} e^{-T} \frac{T^n}{n!},$$

is small. Once n is fixed, the number of required operations to compute the trajectories of M particles is independent of the particle, therefore easily vectorized. The total number of particles $N = N_{loops} \times M$ is computed by N_{loops} successive calculations of packets of M particles.

For a fixed n, the operations required to simulate each trajectory are as follows. We first compute the times at which the process scatters. For each scattering we determine a new velocity k and new polarization parameters q and u of the outgoing particle according to Rayleigh scattering (14) and (15). As seen in (14), the probability distribution of the outgoing velocity depends on the incoming velocity, on the incoming polarization parameters, and on the outgoing velocity. It is however independent of the outgoing polarization parameters. The outgoing polarization parameters are determined by (15) once the outgoing velocity is known. Between scattering events, particles travel along straight characteristic with velocity $v = 1$.

4.2 Spatial and Angular Discretization

Due to the large number of computations needed to simulate each trajectory, we have discretized the velocity and polarization spaces. We precompute the probability distribution of the outgoing parameters for these discrete values of the velocity and polarization. We then replace the exact Rayleigh probability distribution for the outgoing velocity by a piecewise constant probability distribution. Each interaction of a particle with the underlying medium is sampled accordingly.

At the final time the particles must be boxed to do the averaging over the polarization parameters. We discretize the spatial domain with n_x boxes B_i, $1 \leq i \leq n_x$, and the angular domain with n_k directions k_l, $1 \leq l \leq n_k$. Each particle n for $1 \leq n \leq N$, is represented at the final time T by

$(x(n), k(n), q(n), u(n))$, which are its position, velocity, and polarization parameters, respectively. Then for each i and l, we compute the quantities

$$\begin{aligned} I(i,l;T) &= \textstyle\sum_{n=1}^{N} \delta_{in}^{x}\delta_{ln}^{k} \\ Q(i,l;T) &= \textstyle\sum_{n=1}^{N} q(n)\delta_{in}^{x}\delta_{ln}^{k} \\ U(i,l;T) &= \textstyle\sum_{n=1}^{N} u(n)\delta_{in}^{x}\delta_{ln}^{k} \ , \end{aligned} \tag{36}$$

where

$$\delta_{in}^{x} = \begin{cases} 1 \text{ if } x(n) \in B_i, \\ 0 \text{ otherwise,} \end{cases} \qquad \delta_{ln}^{k} = \begin{cases} 1 \text{ if } k(n) \text{ is closer to } k_l \text{ than any other } k_j, \\ 0 \text{ otherwise.} \end{cases} \tag{37}$$

The quantities of interest are the intensity and the degree of polarization defined for each box by

$$I(i;T) = \frac{1}{N}\sum_{l=1}^{n_k} I(i,l;T), \tag{38}$$

$$\alpha_1(i;T) = \frac{\sum_{l=1}^{n_k}\sqrt{Q(i,l;T)^2 + U(i,l;T)^2}}{\sum_{l=1}^{n_k} I(i,l;T)}. \tag{39}$$

5 Numerical Results

In this section, we present numerical solutions of the matrix-valued radiative transfer equation (9), where multiple scattering is taken into account. We first consider the case of non polarized spherical radiation generated by a delta source term. Then, we analyze the same radiation in a half space geometry and examine the behavior of the degree of polarization when interfaces are present.

5.1 Spherical Geometry

5.1.1 Invariance by Rotation and algorithm

The boxing described in Section 4.2 does not take into account the specificities of the spherical geometry. Even though the intensity has to be rotation invariant, this is not true for the polarization parameters, which are given in a basis that is not rotation invariant. The change of polarization parameters under rotations leaving invariant the direction of propagation has been addressed in [1]. We derive here similar formulas for matrix-valued radiative transfer equations.

In spherical geometry, the invariance by a rotation B is characterized for Maxwell's equations by the relations $E(Bx) = BE(x)$ and $H(Bx) = BH(x)$, where E and H are the electric and magnetic fields, respectively. Using this relation and following the derivation of radiative transfer equations described in [17], we see that the solution of (9) satisfies

$$W(t, Bx, Bk) = A(B, k)W(t, x, k)A^*(B, k), \tag{40}$$

in spherical geometry, where A is a unitary 2×2 matrix whose elements are given by

$$A_{ij}(B, k) = (z^{(i)}(Bk), Bz^{(j)}(k)). \tag{41}$$

Here $z^{(i)}$ is defined in (7). The total intensity is obviously not changed by rotation. Following (40), the polarization parameters Q' and U' after rotation are related to Q and U before rotation, by

$$\begin{pmatrix} Q' \\ U' \end{pmatrix} = \begin{pmatrix} A_{11}^2 - A_{12}^2 & 2A_{11}A_{12} \\ -2A_{11}A_{12} & A_{11}^2 - A_{12}^2 \end{pmatrix} \begin{pmatrix} Q \\ U \end{pmatrix}. \tag{42}$$

For every particle n, we use a rotation B such that $Bx(n)$ is parallel to e_z and $Bk(n)$ is in the plane (e_x, e_z). Then, every particle is characterized by its radius and the angle between x and k. After transformation (42), the polarization parameters are expressed in the same basis for every particle, and the averaging can be performed. The boxing (36) now holds for boxes B_i being intervals and directions k_l being angles between 0 and π. It can be shown theoretically that $U \equiv 0$ in spherical geometry for unpolarized sources. This is confirmed numerically.

Equation (39) simplifies then to

$$\alpha_1(r, t) = \frac{\sum_{l=1}^{n_k} |Q(r, k_l, t)|}{\sum_{l=1}^{n_k} I(r, k_l, t)}. \tag{43}$$

The decomposition in the number of scattering events (34) allows us to implement the following algorithm. We deduce from equation (34) that the time dependence of the radiative transfer solution $P(T, z, dz; z_0)$ comes from the weights $Pr(T, N_s = n)$, and that the terms $P(T, z, dz; z_0 | N_s = n)$, like for single scattering where $n = 1$, are actually only functions of $\nu = t/r$ in spherical geometry. We therefore write the degree of polarization as

$$\alpha_1(r,t) = \frac{\sum_{l=1}^{n_k} |\sum_n e^{-t} t^n (n!)^{-1} Q_n(t/r,k)|}{\sum_{l=1}^{n_k} \sum_n e^{-t} t^n (n!)^{-1} I_n(t/r,k)}, \tag{44}$$

where Q_n and I_n are the Stokes parameters obtained for particles that have been scattered n times exactly. This method offers the advantage that we only need to compute $I_n(\nu)$ and $Q_n(\nu)$, for $n = 1, \ldots, N_{max}$, in order to obtain the solution for all times, which are not too large so as to allow us to neglect particles having more than N_{max} scattering events. Note that we can use the exact solution (25) for the first scattering in the summation.

5.1.2 Numerical simulations

We present in Figure 6 the spatial distribution of the degree of polarization and of the intensity for particles having exactly 1, 2, 4, and 8 scattering events. We have observed numerically that the sign of Q_n is independent of n and of the direction k_l. Therefore, depolarization takes place not because the terms corresponding to different numbers of scattering cancel with each other, but because Q_n is a decreasing function in n; see Figure 6(a). Notice however, that the decay in n is relatively slow, and that particles are still approximately 20% polarized for r/t around 0.7 after eight scatterings.

We have represented in Figure 7 the space and time dependent degree of polarization $\alpha_1(r,t)$ obtained by using (44). The spatial distribution of the degree of polarization is shown in Figure 7(a) for different times. For the sake of the comparison we have rescaled the total distance to 1 for the direct arrival for all times. We have plotted in Figure 7(b) time traces of the same quantity $\alpha_1(r,t)$ for different distances to the source r_s. We have also rescaled time such that $t = 1$ always corresponds to the direct arrival. We observe that the degree of polarization vanishes at $r = 0$, where the light is thus unpolarized, and that it has one identifiable maximum. When multiple scattering is taken into account, this maximum is now a function of time in contrast with the single scattering approximation. The maximum as a function of the distance to the location of the source term is plotted in Figure 8(a). We observe that it decreases relatively slowly with the distance and eventually vanishes for large distances. The position t_{max}/r of this maximum also depends on the distance to the source. Nevertheless, we can see in Figure 8(b) that the position of the peak has changed by at most 15% when the energy is received at a distance $r = 8$ mean free paths away from the unpolarized source. Thus, Figure 8 can be used to estimate the distance separating the source from far receivers, assuming that the velocity of propagation –equal to 1 in our simulations– is

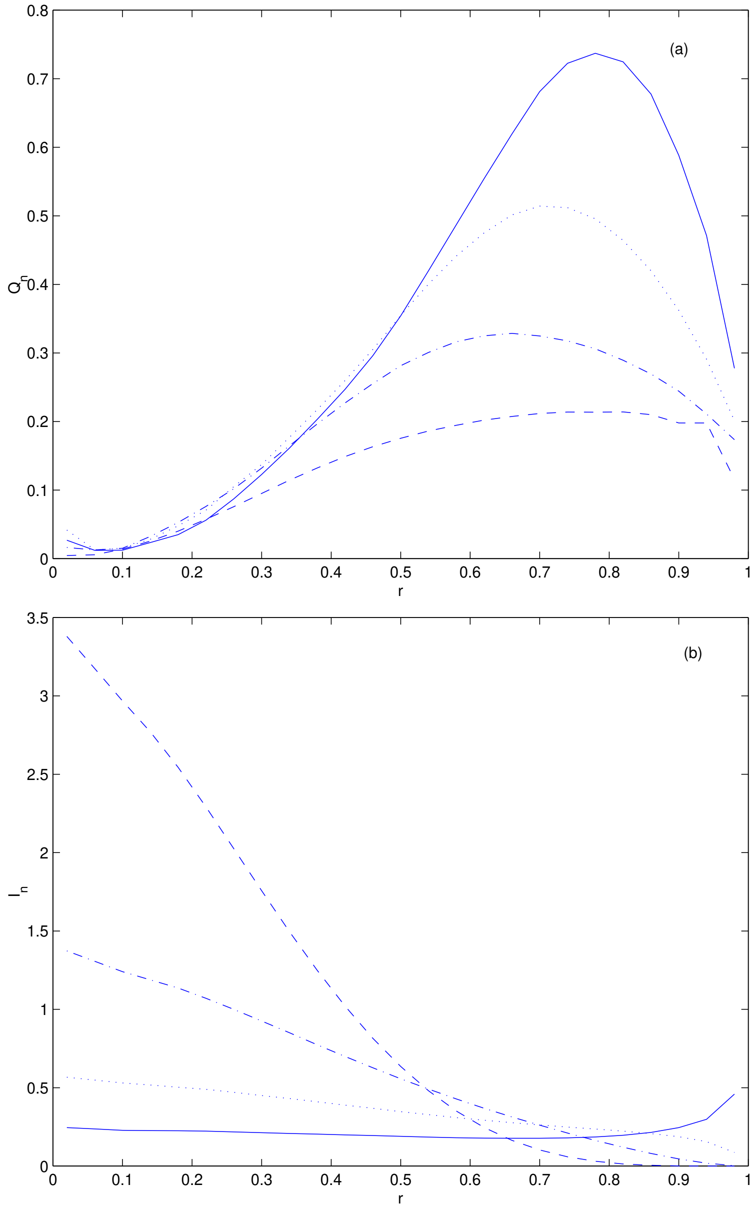

Fig. 6. Spatial distribution of (a) the degree of polarization and (b) the intensity of particles having 1 (solid line), 2 (dotted line), 4 (dash-dotted line) and 8 (dashed line) scattering events.

known.

Let us emphasize the main conclusion we can draw from these computations. Even far away from the source, the light remains to a large extent polarized. The process of depolarization due to multiple scattering is very slow. The reason is that multiple scattering, which is indeed responsible for the depolarization, is mainly concentrated in the vicinity of the source [see Figure 6(b)]. Moreover, the multiply scattered particles that escape this area and approach the ballistic front, in addition to being rare, follow very specific paths. This

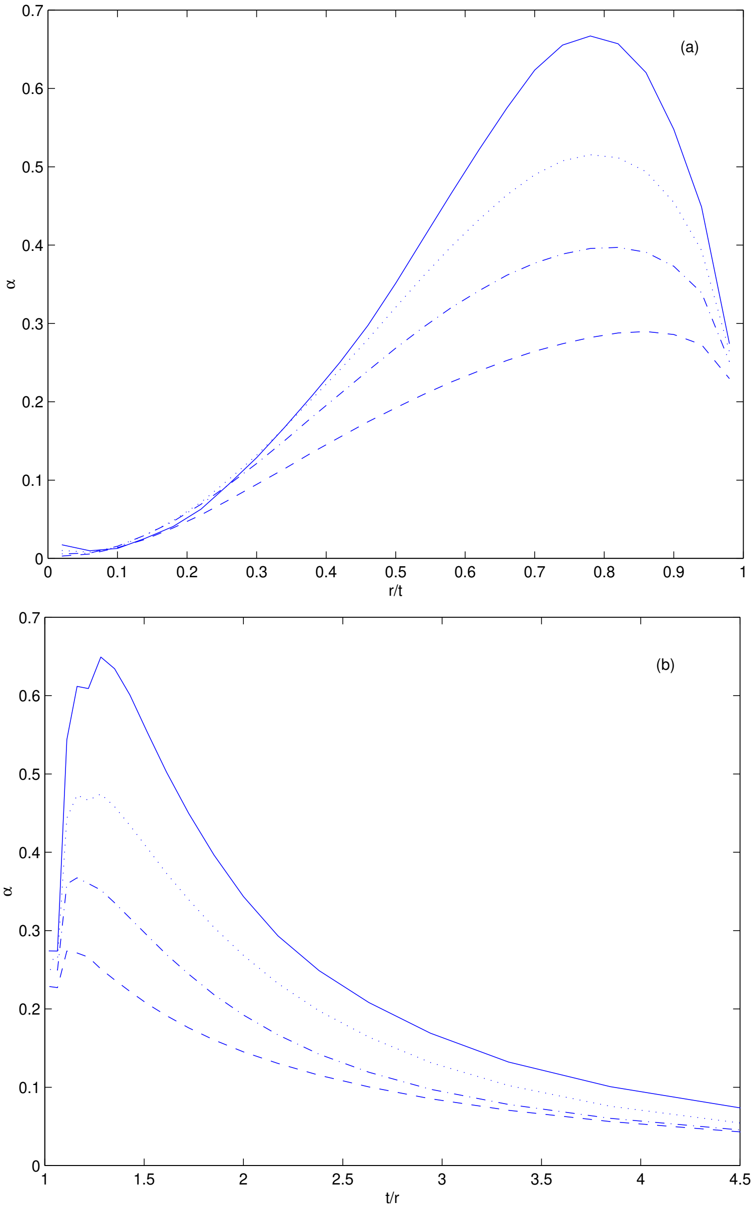

Fig. 7. Spatio-temporal change in the degree of polarization. (a) Spatial distribution at times $t = 0.5, 2, 4$ and 8. (b) Time evolution at distances $r_s = 0.5, 2, 4$ and 8 to the source.

behavior is caused mainly by the convection term $\hat{k} \cdot \nabla W$ in the radiative transfer equation and is qualitatively very different from the homogeneous case treated in Section 3.2. We also mention similar results showing the relatively slow decay of polarization for polarized narrow beams of light incident on a plane-parallel scattering medium [4].

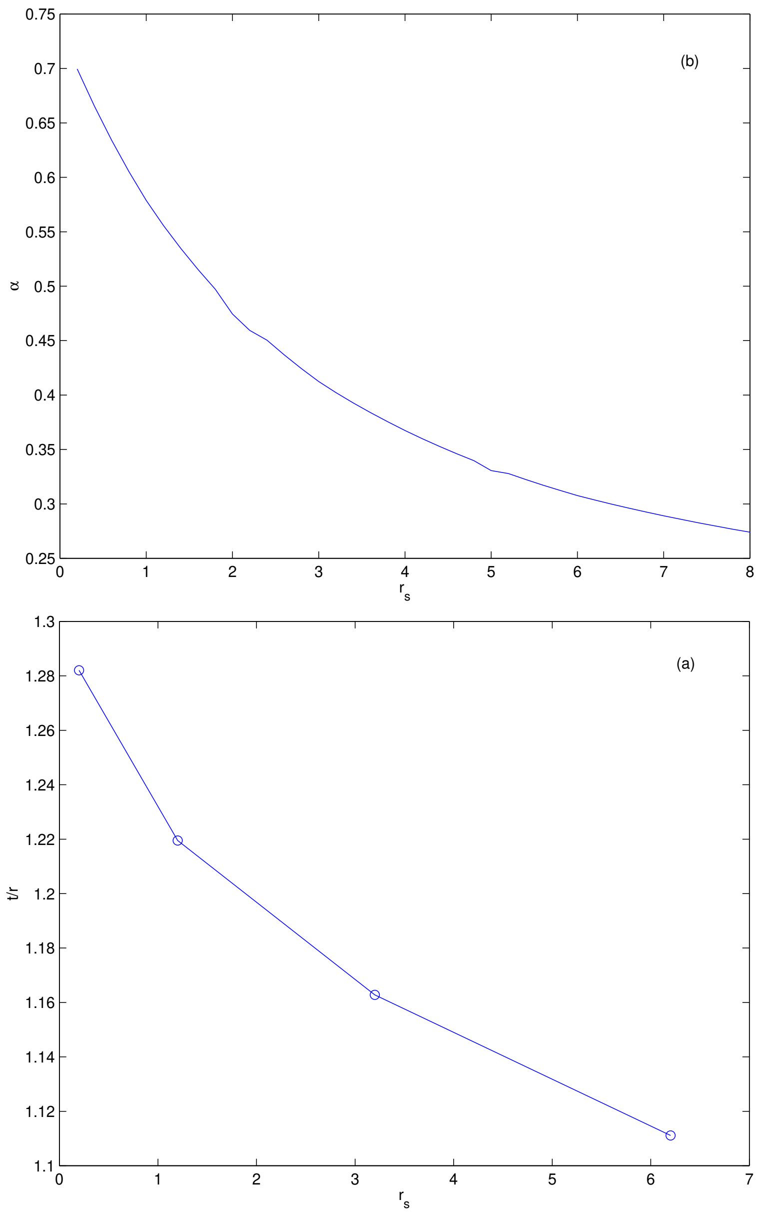

Fig. 8. Dependence on the distance to the source of (a) the maximum of the degree of polarization and (b) the position of this maximum.

5.2 Half Space Geometry

We consider in this section the more general, albeit still simple, problem of an isotropic delta source term in half space. We want to analyze the effect of a horizontal perfectly reflecting boundary on the degree of polarization.

Even though we do not have rotational invariance anymore, we still have cylindrical invariance around the z axis. Therefore, once the position, velocity, and polarization parameters are computed, we can rotate that particle so as to bring it in the plane xz, say. Such a rotation leaves the polarization parameters invariant. Indeed, if B_ϕ is a rotation around the z axis, then we have $B_\phi[z^{(i)}(k)] = z^{(i)}(B_\phi[k])$, where $z^{(i)}$ is defined in (7). After rotation, a particle is described by its vertical coordinate z, its distance to the z-axis r, and its velocity k_l, where the directions k_l form a discretization of the unit sphere. For each direction k_l, we store the particles in boxes B_{ij} centered around points r_i and z_j, where

$$r_i = i\Delta r, \qquad i = 1, \ldots, n_r, \tag{45}$$

$$z_j = z_{min} + j,\ \Delta z \qquad j = 1, \ldots, n_z. \tag{46}$$

Here, z_{min} is the minimal z that can be reached by the particles, and Δr and Δz are the sizes of the uniform grids in r and z, respectively.

We have represented in Figure 9 the degree of polarization $\alpha_1(r, z; t)$ for time $t = 2$. The non-polarized isotropic point source is located at distance $z = 1$ from the interface. We can clearly separate the domain (r, z) in two areas. The lower part is actually identical to the spherical symmetry case. The maximum of the degree of polarization, around 0.5, agrees perfectly with the one shown in Figure (7) at time $t = 2$. The upper part corresponds to the area where the energy has been partially reflected from the interface. We observe that the degree of polarization is lower than in spherical geometry. This is due to the fact that the polarization of the reflected part adds destructively to that part which did not see the interface.

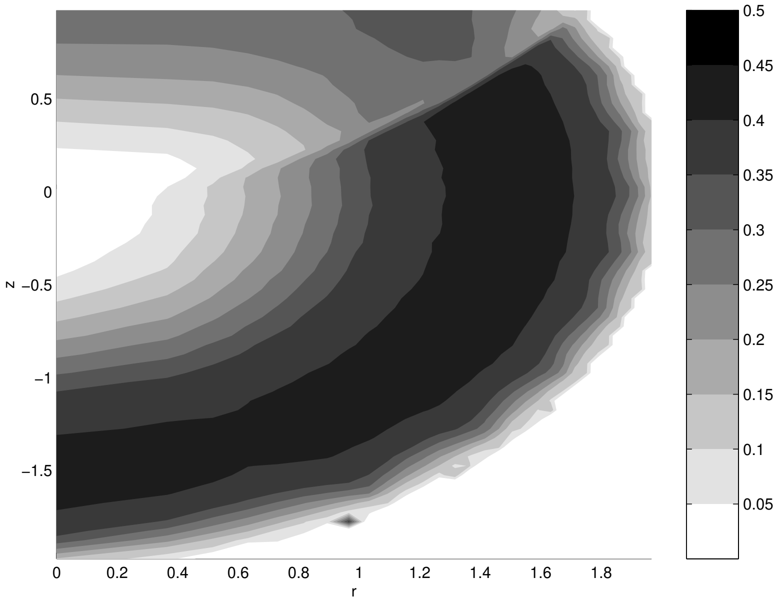

Fig. 9. Degree of polarization in the half space geometry. The non polarized isotropic point source is at $z = 0$ and the free surface is at $z = 1$.

More interesting is the value of the degree of polarization at the surface, where it can be easily measured. In Figure 10 we see that, in spite of the relative diminution of the polarization caused by the interface, an observer will detect an significant amount of polarized energy during early times. As in the spherical geometry, the degree of polarization starts from zero, then grows until it quickly reaches a maximum, and then slowly decreases back to zero for large times.

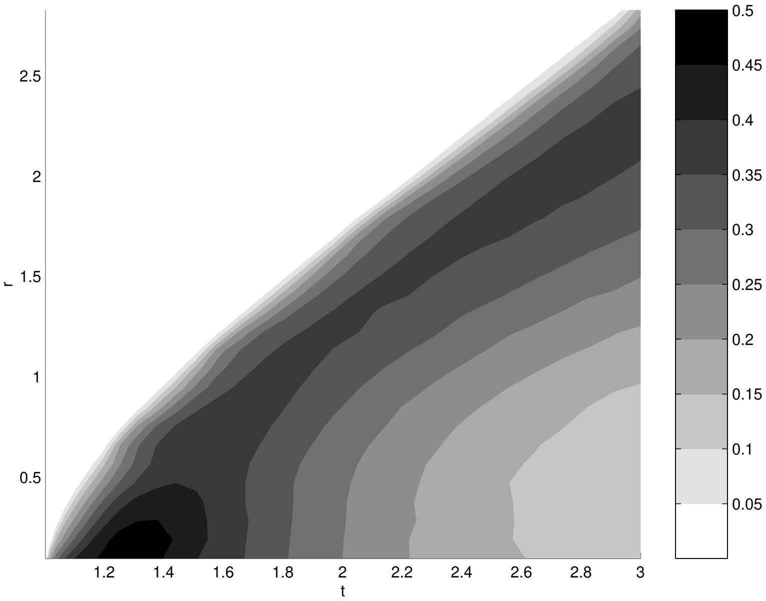

Fig. 10. Degree of polarization pattern at the surface. The non polarized isotropic point source is at a distance 1 from the surface.

To summarize, we can infer from our numerical computations that the perfectly reflecting boundary causes a decay in the rate of polarization but does not cancel it. The rate of polarization remains definitely observable, and may be used as an additional piece of information in order to solve inverse problems more accurately.

6 Conclusions

We have studied in this paper the polarization and depolarization effects of matrix-valued radiative transfer problems. We have calculated analytically the intensity and degree of polarization for single scattering with a spherically radiating natural source. We have seen that in this setting, up to 80% of the initially unpolarized light becomes polarized after first scattering. The maximum of polarized light as a function of time for a fixed position r, even when low order multiple scattering in taken into account, is obtained for a value close to $t \approx 1.27r$ with unit speed; which could be used as a rough estimate of the distance between the receiver and the point source. We also have seen that polarization appears quickly and that depolarization is very slow. More than 8 scattering events are required to observe a rate of polarization below 20%. For half-space problems, we have shown that the presence of an interface lowers the degree of polarization significantly due to polarization cancellations. However, the degree of polarization remains clearly observable. We have presented Monte Carlo simulations based on a probabilistic representation of polarized radiative transfer equations. Even though only elementary geometries were treated here, the same method can be used for more complicated geometries and more general boundaries or interfaces, such as those derived in [25] for instance.

Acknowledgment

We would like to thank Joseph B. Keller, George Papanicolaou and Leonid Ryzhik for valuable comments and advice during the preparation of this paper. This work was supported by AFOSR grant 49620-98-1-0211 and by NSF grant 9709320.

A Scattering Matrix for Rayleigh Scattering

We give here an explicit expression for (14) and (15) in the case of Rayleigh scattering. The components of the T matrix (6) are given by

$$\begin{aligned} T_{11} &= \cos\theta_k \cos\theta_{k'} \cos(\phi_k - \phi_{k'}) + \sin\theta_k \sin\theta_{k'}, \\ T_{12} &= \cos\theta_k \sin(\phi_k - \phi_{k'}), \\ T_{21} &= \cos\theta_{k'} \sin(\phi_{k'} - \phi_k), \\ T_{22} &= \cos(\phi_k - \phi_{k'}). \end{aligned} \tag{A.1}$$

Upon expanding the trace of TWT^*, we have

$$\Pi(k, \mathcal{P}, k', \mathcal{P}') = \frac{3}{8\pi}\Big[\frac{T_{11}^2 + T_{21}^2}{2}(1+p_1) + \frac{T_{12}^2 + T_{22}^2}{2}(1-p_1) + (T_{11}T_{12} + T_{21}T_{22})p_2\Big]. \tag{A.2}$$

Then we obtain from (15)

$$p'_1 = \frac{8\pi}{3\Pi(k,\mathcal{P},k',\mathcal{P}')}\Big[\frac{T_{11}^2 - T_{21}^2}{2}(1+p_1) + \frac{T_{12}^2 - T_{22}^2}{2}(1-p_1) + (T_{11}T_{12} - T_{21}T_{22})p_2\Big]$$
$$p'_2 = \frac{8\pi}{3\Pi(k,\mathcal{P},k',\mathcal{P}')}\Big[T_{11}T_{21}(1+p_1) + T_{12}T_{22}(1-p_1) + (T_{11}T_{22} + T_{12}T_{21})p_2\Big]. \quad \text{(A.3)}$$

B Single Scattering Intensity and Polarization

Let us derive here equations (24) and (25).

The intensity which arrives at a point $\mathbf{r}$ after scattering at $\mathbf{r_1}$ under the Rayleigh's law is [see Figure 1]:

$$\frac{1}{4\pi r_1^2}\frac{1}{4\pi r_2^2}\frac{3}{4}(1+\cos^2\Theta)\ . \quad \text{(B.1)}$$

The factors $1/4\pi r_1^2$ and $1/4\pi r_2^2$ in (B.1) come from the geometrical spread of the intensity from the source to the scatter and from this to the receiver, respectively. To obtain the total intensity at time t we have to integrate over all the space under the condition that the total travel time of the light is equal to t. Then,

$$I(\mathbf{r},t) = \frac{3}{(8\pi)^2}\int \frac{1}{r_1^2 r_2^2}(1+\cos^2\Theta)\delta(t-r_2-r_1)d\mathbf{r_2} = \quad \text{(B.2)}$$
$$\frac{3}{(8\pi)^2}\int_0^\infty\int_0^\pi\int_0^{2\pi}\frac{\delta(t-r_2-r_1)}{r_1^2 r_2^2}(1+\cos^2\Theta)r_2^2 dr_2 sin\varphi d\varphi d\phi\ .$$

Let us remark that

$$\begin{aligned}\delta(t-r_2-r_1) &= 2r_1\delta((t-r_2)^2-(r_1)^2)\\ &= 2r_1\delta((t-r_2)^2-2r_2(t-r\cos\varphi))\\ &= \frac{r_1}{t-r\cos\varphi}\delta(r_2-\frac{t^2-r^2}{2(t-r\cos\varphi)}).\end{aligned}$$

Therefore, we have

$$I(r,t) = \frac{3}{32\pi}H(t-r)\int_0^\pi \frac{1}{r_1(t-r\cos\varphi)}(1+\cos^2\Theta)sin\varphi d\varphi, \quad \text{(B.3)}$$

which yields (24). The numerator in (23) is the same as in (B.3) except for the positive sign in front of $\cos^2\Theta$ replaced by a negative sign.

To integrate (B.3) it is more convenient to change to prolate spheroidal coordinates (ν, ω, ϕ) as in [16]. The change of variables is the following:

$$x = \frac{r}{2}\sqrt{(\nu^2-1)(1-\omega^2)}\cos\phi \; y = \frac{r}{2}\sqrt{(\nu^2-1)(1-\omega^2)}\sin\phi \; z = \frac{r}{2}(1+\nu\omega) \; . \quad \text{(B.4)}$$

where r is the distance between the source and the receiver, and $\omega \in [-1, 1]$, $\nu \in [1, \infty)$ and $\phi \in [0, 2\pi]$. The Jacobian of this transformation is $\frac{r r_1 r_2}{2} d\nu d\omega d\phi$ and

$$\cos\Theta = \frac{2-\nu^2-\omega^2}{\nu^2-\omega^2} \; . \quad \text{(B.5)}$$

With these relations we end up with the integration of a rational function which can be performed trivially. The result is equation (26). Equation (25) can be done similarly.

References

[1] S. Chandrasekhar. *Radiative Transfer.* Dover Publications, New York, 1960.

[2] A. Ishimaru. *Wave Propagation and Scattering in Random Media.* New York: Academics, 1978.

[3] H. C. van de Hulst. *Multiple Light Scattering.* Academic Press, New York, NY, 1980.

[4] A. Ambirajan and D.C. Look. A Backward Monte Carlo Study of the Multiple Scattering of a Polarized Laser Beam. *J. Quant. Spectrosc. Radiat. Transfer*, 58 No.2:171–192, 1997.

[5] M.I. Mishchenko, A.A. Lacis, and L.D. Travis. Errors induced by the neglect of polarization in radiance calculations for rayleigh-scattering atmospheres. *J. Quant. Spectrosc. Radiat. Transfer*, 51, No.3:391–510, 1994.

[6] G. C. Pomraning. A Renormalized Equation of Transfer for Rayleigh-Scattering. *J. Quant. Spectrosc. Radiat. Transfer*, 60:181–197, 1998.

[7] H. R. Gordon, J. W. Brown, and R. H. Evans. Exact Rayleigh scattering calculations for use with the nimbus-coastal zone color scanner. *Appl. Opt.*, 27:862, 1988.

[8] S. Mukai. Atmospheric correction of remote sensing images of the ocean based on multiple scatering calculations. *IEEE Trans. Geosci. Remote Sens.*, 28:696, 1990.

[9] S. G. Demos and R. R. Alfano. Optical polarization imaging. *Applied Optics*, 36:150–155, 1997.

[10] B. C. Wilson and G. Adam. A monte carlo model for the absorption and flux distributions of light in tissue. *Med. Phys.*, 10:824, 1983.

[11] A. Bensoussan, J.-L. Lions, and G. Papanicolaou. Boundary layers and homogenization of transport processes. *Res. Inst. Math. Sci., Kyoto Univ.*, 15:53–157, 1979.

[12] M. H. Kalos and P. A. Whitlock. *Monte Carlo Methods.* J. Wiley and sons, New York, 1986.

[13] J. Spanier and E. M. Gelbard. *Monte Carlo principles and neutron transport problems.* Addison-Wesley, Reading, Mass., 1969.

[14] G. Bal, G. Papanicolaou, and L. Ryzhik. Probabilistic Theory of Transport Processes with Polarization. *SIAM Appl. Math.*, 60(5):1639–1666, 2000.

[15] K. M. Yoo and R. R. Alfano. Time Resolved Depolarization of Multiple Backscattered Light from Random Media. *Phys. Lett. A*, 142:531–536, 1989.

[16] H. Sato and M. C. Fehler. *Seismic wave propagation and scattering in the heterogeneous earth.* AIP series in modern acoustics and signal processing. AIP Press, Springer, New York, 1998.

[17] L. Ryzhik, G. Papanicolaou, and J. B. Keller. Transport equations for elastic and other waves in random media. *Wave Motion*, 24:327–370, 1996.

[18] H. C. van de Hulst. *Light Scattering by Small Particles.* Dover, New York, 1981.

[19] C. F. Bohren and D. R. Huffman. *Absorption and Scattering of Light by Small Particles.* Willey, New York, 1983.

[20] D. Bicout, C. Brosseau, A. S. Martinez, and J. M. Schmitt. Depolarization of multiply scattered waves by spherical diffusers: influence of the size parameter. *Phys. Rev. E*, 49:1767–1770, 1994.

[21] P. C. Y. Chang, J. G. Walker, E. Jakeman, and K. I. Hopcraft. Polarization properties of light multiply scattered by non-spherical Rayleigh particles. *Waves Rand. Med.*, 9:415–426, 1999.

[22] G. Bal and M. Moscoso. Polarization Effects of Seismic Waves on the Basis of Radiative Transport Theory. *Geophys. J. Int.*, 142(2):571–585, 2000.

[23] E. W. Larsen and J. B. Keller. Asymptotic solution of neutron transport problems for small mean free paths. *J. Math. Phys.*, 15:75–81, 1974.

[24] J. Neveu. *Introduction aux Probabilités.* Cours Ecole Polytechnique, 1992.

[25] G. Bal, J.B. Keller, G. Papanicolaou, and L. Ryzhik. Transport theory for waves with reflection and transmission at interfaces. *Wave Motion*, 30:303–327, 1999.